On the Nature of Dynamic Interference Fringes Excited by Coherent Beam

Chandan Siam

***Abstract*—The present work reports the interpretation of circular fringes appearing on a screen at a suitable distance from a sample cell when coherent beam of light (He-Ne Laser, Ar^+ Laser) of suitable power is incident on it. The dynamic fringes are characteristics of liquids used in the experiment. In the present work we have shown that these fringes are originated from suspended particles in the liquid. We have also estimated the sizes of the particles. The characteristic of the fringes follows Maxwell-Boltzmann type of distribution.**

***Index Terms*—Dynamic fringes, diameter and speed of suspended particles.**

I. Introduction

The work is focused on the description of the dynamics of the circular fringes in different experimental conditions. It is worthwhile to indicate here that the methods used here are relatively simple. Light diffraction by small particles carried in a liquid flow has not been extensively studied though Laser Anemometry as applicable to fluid flow has been studied for many years [1]-[3]. References on the subject of dynamic fringes as discussed are surprisingly missing from the literature. Therefore our study on the dynamic fringes is based on the simple experimental observations which we have carried out and our observations are independent of any ideas and belief that may have existed in the past. But there are relative literatures dealing with moving fringes in photorefractive polymers [4]-[10]. The use of the moving interference patterns created using the angular Doppler Effect has been found to control lateral and rotational movement of trapped particles [11]-[24]. Some literatures dealing with the phenomena of the evolution of the interference fringes may also be found in some recent literatures [25]-[28].

II. Experimental Process

The experimental arrangement used in the present work is shown schematically in Fig. 1. He-Ne(5mW-6328Å) or Ar^+ laser(500mW-5145Å) laser is incident on the lower part of a cylindrical test tube containing a particular liquid, which is transparent, and also relatively dust free. Moving fringes are projected on the screen at a distance of 2m to 4m away from the sample tube. The fringes are projected in a certain condition that the laser light must be incident in the lower part of the test tube where the test tube is oval in shape. These fringes are created at a particular point and move in a particular direction without undergoing any change in shape. We have used a video camera (model-DCR-TRV460E-Sony) to record these events of dynamic fringes for several hours and the images are transferred to a computer. Also we get moving fringes in torch bulb and liquid drop instead of a test tube. Fig. 2 and Fig. 3 show the moving fringes using He-Ne laser and Ar^+ laser respectively; arrowheads indicate the moving fringes.

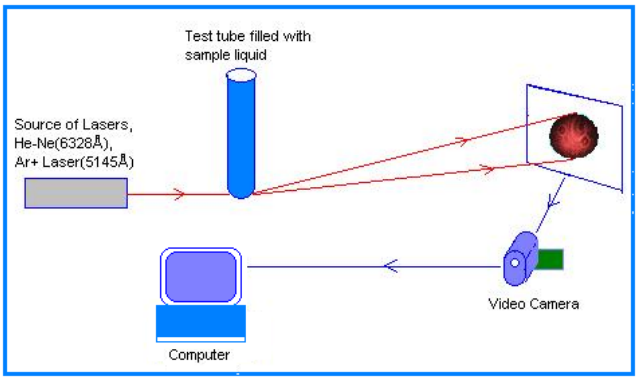

Fig. 1. Experimental setup for moving fringes.

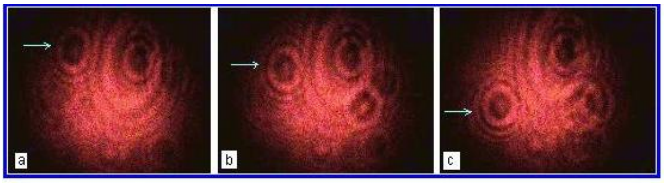

Fig. 2. Three photographs(a, b, c) of a moving fringe at different positions observed using He-Ne laser, the arrowed indicate the different positions of the moving fringe.

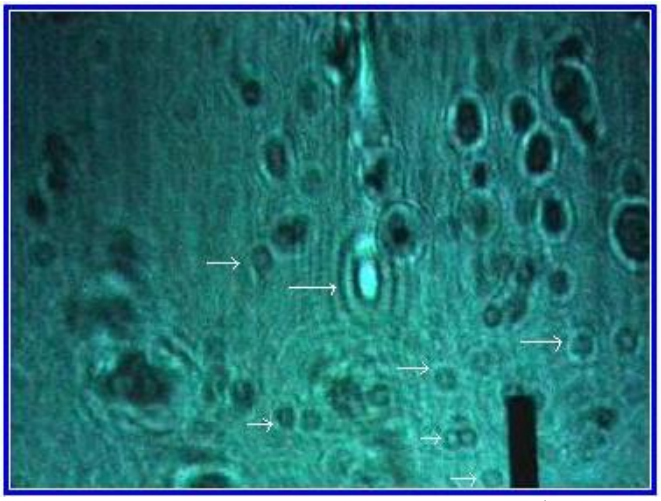

Fig. 3. A photograph of moving fringes observed using Ar^+ Laser, arrowheads indicate the moving fringes.

The fringes are moving in various directions with different speeds. In the vector diagram (Fig. 4) each arrowhead

Manuscript received December 3, 2013; revised February 28, 2014.
Chandan Siam is with Physics Department, Digboi College, Digboi-787001, Assam, India (e-mail: csiam162@gmail.com)

indicates the direction of movement of a fringe. The directions of velocities are worked out for acetone from the computer displaying in windows media player for duration of four minutes.

Direction of moving fringes:

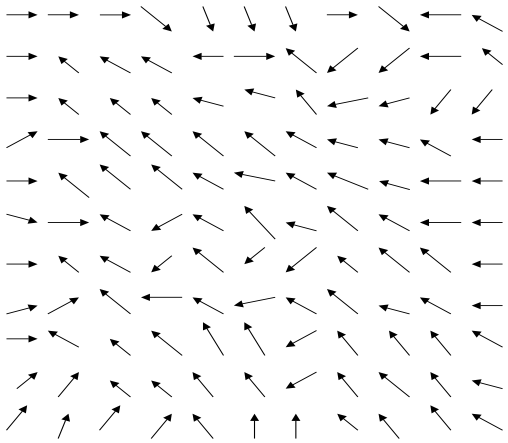

Fig. 4. Arrowhead diagram of moving fringes.

III. Speeds of Moving Fringes

The moving fringes are projected on a screen, 2m to 4m distances from the sample cell. The images of the moving fringes (Fig. 2, Fig. 3) are recorded by video camera and displaying in a computer, using *vcd cutter* software we calculated the speed of each fringe in the unit of mm/sec and cm/sec. Using scale factor we measure the actual speed of moving fringes inside the liquids in the unit of m/sec. The speeds of the fringes in m/sec versus the number of fringes exhibit distributions; which are analogous to Maxwell – Boltzman type of distributions. This is shown in Fig. 5 (a, b, c,……..l) for different liquids.

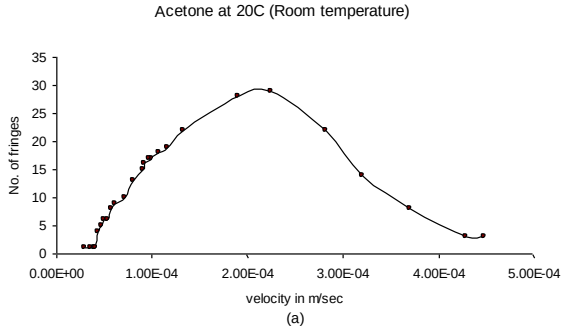

Fig. 5 (a). The speed distribution curves, obtained by plotting the speed of the fringes(m/sec) versus the number of fringes of acetone.

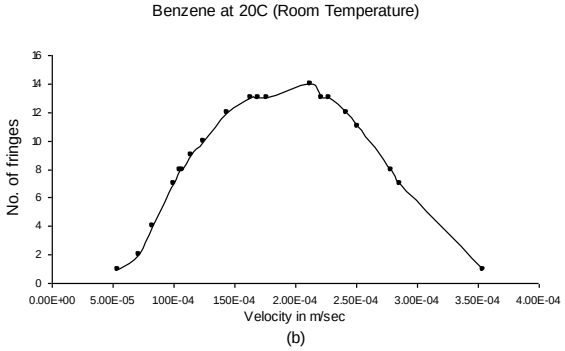

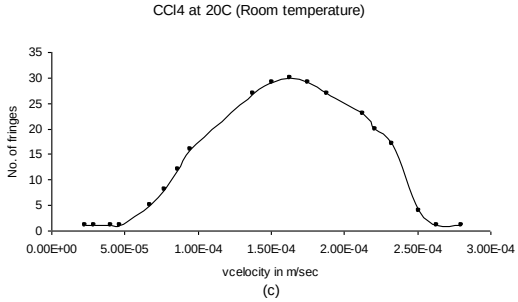

Fig. 5 (b, c). The speed distribution curves, obtained by plotting the speed of the fringes(m/sec) versus the number of fringes of Benzene and CCl_4.

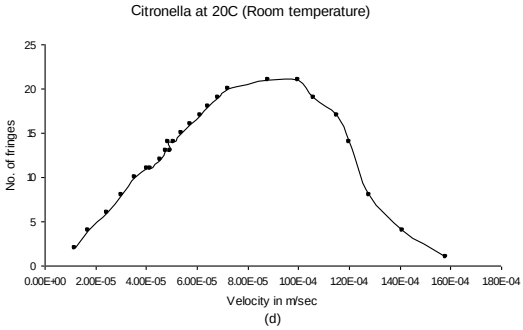

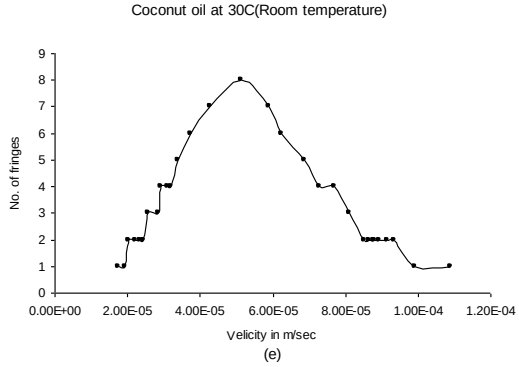

Fig. 5 (d, e). The speed distribution curves, obtained by plotting the speed of the fringes(m/sec) versus the number of fringes of Citronella and Coconut oil.

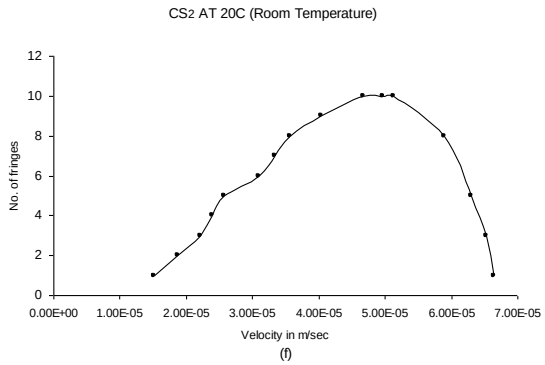

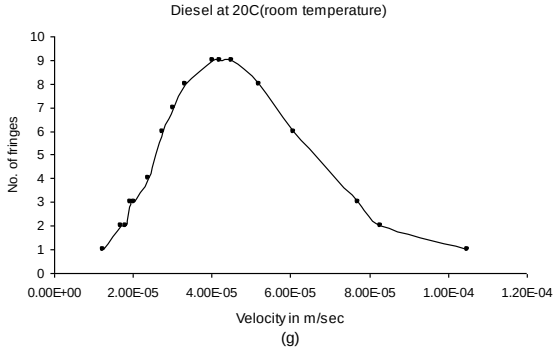

Fig. 5 (f, g). The speed distribution curves, obtained by plotting the speed of the fringes(m/sec) versus the number of fringes of CS_2 and Diesel.

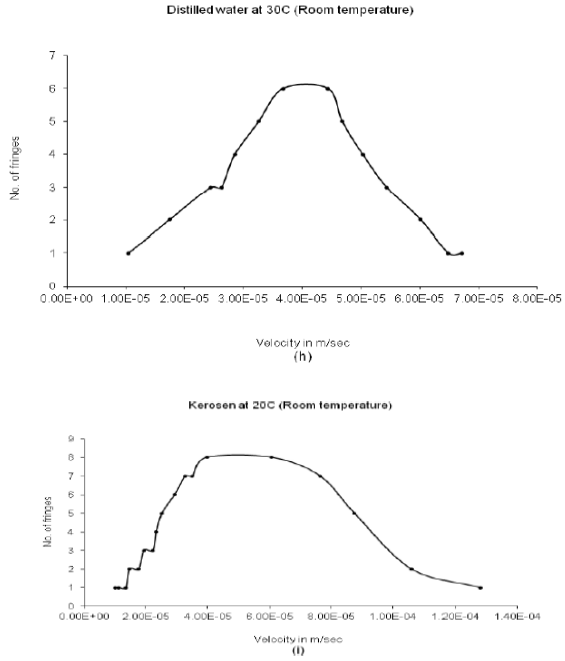

Fig. 5 (h, i). The speed distribution curves, obtained by plotting the speed of the fringes(m/sec) versus the number of fringes of Distilled water and Kerosen.

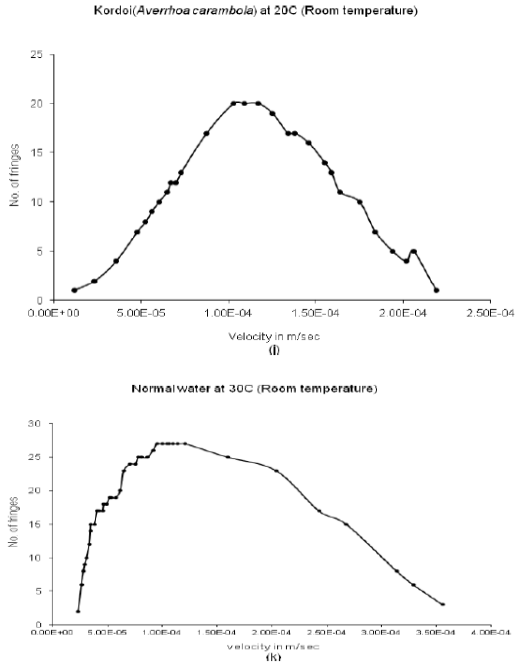

Fig. 5 (j, k). The speed distribution curves, obtained by plotting the speed of the fringes(m/sec) versus the number of fringes of Averrhoa Carambola and Normal water.

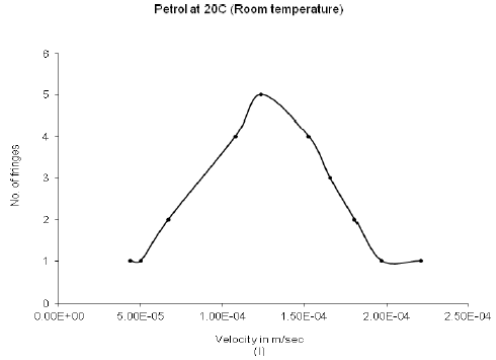

Fig. 5 (l). The speed distribution curves, obtained by plotting the speed of the fringes(m/sec) versus the number of fringes of Petrol.

IV. Origin of Moving Fringes

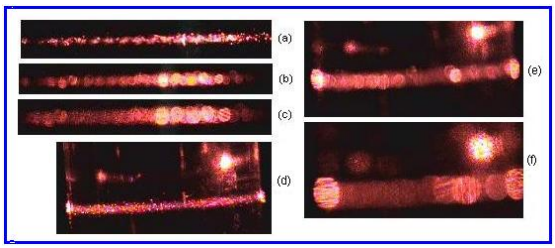

Fig. 6. Images of particles or air bubbles or colloids in the path of laser beam in glass strip and in liquids. (a, b, c)- inside the glass strip; (e, f, g)-inside the liquid.

Both the Fig. 6 (a, d) are similar, without zooming the video camera we get these images in the path of laser beam in glass strip and in liquids. Actually glass is a super cooled liquid, in case of glass, the images are static, but in liquids, the images are dynamic. With our necked eyes, in the path of laser beam images are seen as point source of light as stars in the sky in night. After proper zooming the video camera, we get the images as shown in Fig. 6 (b, c) in glass strip and in Fig. 6 (e, f) in liquid, round in shape like disc. In liquids the point sources as well as the disc images are moving, our experimental system projects the magnified images to the screen. The images are fringes round in shape observed on the screen.

V. Projection Theory of Moving Fringes

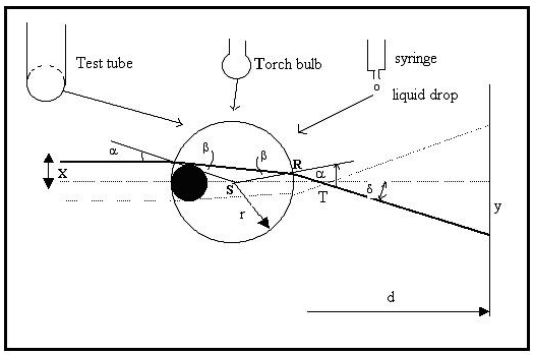

Fig. 7. Schematic diagram of projection of moving fringe.

The lower part of the test tube (Fig. 7), when filled with liquid is a part of a perfect sphere can be treated as a small spherical lens like water drop [29], [30] or torch bulb. The laser beam that falls on the lower part of the test tube refracts twice times as it passes through the liquid-air interface. Let's follow the path of the ray that enters the liquid just above an object that floats in the liquid at a small distance x from the geometrical axis. The ray will refract twice and reach the screen at the distance y below the geometrical axis. The distance y is determined by the distance from the test tube to the screen d and the angle δ, which can be calculated using simple geometry:

$$\delta = \alpha - \angle RST$$

$$\angle RST = 2\beta - \alpha$$

$$\delta = 2(\alpha - \beta)$$

Using snell's law

$\frac{\sin\alpha}{\sin\beta}=\frac{n}{n_0}$ where for the liquid and air n, and n0=1.0 respectively and with $\sin\alpha=\frac{x}{r}$, the angle δ is given by the equation:

$$\delta = 2(\arcsin\frac{x}{r}-\arcsin\frac{x}{nr})$$

For the rays close to the geometrical axes (paraxial region), all the angles in the calculation above are very small; therefore, the expression for δ can be simplified using the approximation $\arcsin(z)\approx z$

$$\delta = 2\frac{x}{r}(1-\frac{1}{n})$$

The projected image on the screen is a magnified one with magnification equal to

$$M=\frac{y}{x}\frac{d\tan\delta}{x}\approx 2\frac{d}{r}\left(1-\frac{1}{n}\right)$$

where approximation $(\tan\delta\approx\delta)$ is valid in the paraxial region. For the sphere 2mm in diameter, the image on the screen 2m from the setup is about 1000 times larger than the object.

Clearly, the magnification is largest for the surface of the sphere facing the screen. In this case in paraxial region

$$M_{\max}=\frac{d}{2r}\frac{n}{2-n} \quad (1)$$

For the parameters given above, the magnification factor is 1985.

The results show that in the paraxial region, the magnification depends on the position of the object along the geometrical axis but not on the object's distance from the axis.

VI. Evaluation of Actual Diameter of Moving Fringes

For a particle floating in the screen side of the tube the magnification is given by, from equation (1)

A. Using Ar + Laser

$$m=\frac{d}{2r}\frac{n}{2-n}$$

where *d* is the distance of the tube from the screen, r is the radius and n is the refractive index of the liquid. Using the value *d*=600cm, *r*=0.5cm and *n*=1.3(water) the magnification factor is 1800.

TABLE I: Evaluation of Actual Diameters of Moving Fringes in Micro-Meter

Fringe diameter on computer screen (mm)	(Scale factor 1:10) Fringe diameter on projection screen (mm)	Actual diameter of fringes (Scale factor 1:1800) (mm)	In μm
5	50	50/1800=0.02777	27.77
6	60	60/1800=0.03333	33.33
10	100	100/1800=0.05555	55.55
4	40	40/1800=0.02222	22.22
4.5	45	45/1800=0.025	25.00
3.5	35	35/1800=0.01944	19.44
3	30	30/1800=0.01666	16.66
5.5	55	55/1800=0.03055	30.55
6.5	65	65/1800=0.03666	36.66
7	70	70/1800=0.03888	38.88
7.5	75	75/1800=0.04166	41.66
8	80	80/1800=0.04444	44.44
8.5	85	85/1800=0.04722	47.22
9	90	90/1800=0.05	50.00
9.5	95	95/1800=0.05277	52.77

B. Using He-Ne Laser

Using the value *d*=400cm, *r*=0.5cm and *n*=1.3(water) the magnification factor is 1200

C. Evaluation of Diameters of Suspended Particles or Air Bubbles in Liquids

In acetone, we observe moving fringes continuously, but, when the liquid is disturbed with a twig, we observe more number of moving fringes. In other liquids also, similar phenomenon are observed. In case of water, when a small amount of Na_2CO_3 is introduced into the test tube, the water is polluted with air bubbles or particles, then, we observe more number of moving fringes. The particles or air bubbles or colloids suspended in liquids continuously move to and fro are projected to screen as moving fringes. Therefore, the moving fringes are the manifestation of the suspended particles or air bubbles or colloids in liquids. We measured the speed of fringes in computer monitor using suitable software in mm/sec or cm/sec, with the help of scale factor and equation (1), calculated the actual speeds inside liquids.

The well known equation of suspended particles in liquids

$$R=\left(\frac{9\eta v}{2(\rho_2-\rho_1)g}\right)^{1/2}.$$

Here, R-radius of particles or air bubbles or colloids in average. η-co-efficient of viscosity, ρ_2-density of particles, bubbles or colloids, ρ_1-density of vehicle liquids, g-acceleration due to gravity, v-speed of moving fringes.

We evaluated the sizes of particles or air bubbles or colloids suspended in liquids as shown in following tables (1 to 12). Actual density of particles, or colloids suspended in liquids are not known, hence, we evaluated diameters for the density ranges (ρ_2 -ρ_1)=1500kg/m^3, 2500 kg/m^3, 3500 kg/m^3, 4500 kg/m^3. In the first column of each table we take ρ_1=1kg/m^3 (air density), therefore, it indicates the radius of air bubbles suspended in liquids.

TABLE II: EVALUATION OF ACTUAL DIAMETERS OF MOVING FRINGES IN MICRO-METER

Fringe diameter on computer screen (mm)	(Scale factor 1:7) Fringe diameter on projection screen (mm)	Actual diameter of fringes (Scale factor 1:1200) (mm)	In μm
10	70	70/1200=0.05833	58.33
15	105	105/1200=0.0875	87.50
8	56	56/1200=0.04666	46.66
6	42	42/1200=0.035	35.00

TABLE III: SIZE OF PARTICLES OR AIR BUBBLES OF ACETONE (20^{o}C)

Actual velocity v (m/sec)	(ρ_2 - ρ_1) kg/m^3				
	759	1500	2500	3500	4500
	Radius R (μm)				
2.92E-05	2.38	1.69	1.31	1.1	0.97
3.62E-05	2.65	1.88	1.45	1.23	1.08
3.97E-05	2.77	1.97	1.52	1.29	1.13
4.08E-05	2.81	1.99	1.54	1.3	1.15
4.38E-05	2.91	2.07	1.6	1.35	1.19
4.67E-05	3.01	2.13	1.65	1.4	1.23
5.02E-05	3.12	2.21	1.71	1.45	1.28
5.31E-05	3.21	2.28	1.76	1.49	1.31
5.78E-05	3.35	2.38	1.84	1.55	1.37
6.13E-05	3.44	2.45	1.89	1.6	1.41
7.18E-05	3.73	3.73	2.05	1.73	1.53
7.99E-05	3.93	2.79	2.16	1.83	1.61
9.10E-05	4.2	2.98	2.31	1.95	1.72
9.22E-05	4.22	3	2.32	1.96	1.73
9.74E-05	4.34	3.08	2.39	2.02	1.78
1.00E-04	4.4	3.13	2.42	2.04	1.8
1.07E-04	4.55	3.23	2.5	2.11	1.86
1.16E-04	4.74	3.37	2.61	2.2	1.94
1.33E-04	5.07	3.61	2.79	2.36	2.08
1.90E-04	6.06	4.31	3.34	2.82	2.49
2.25E-04	6.6	4.69	3.63	3.07	2.71
2.82E-04	7.39	5.25	4.07	3.44	3.03
3.20E-04	7.87	5.59	4.33	3.66	3.23
3.70E-04	8.46	6.02	4.66	3.94	3.47
4.28E-04	9.1	6.47	5.01	4.23	3.73
4.48E-04	9.31	6.62	5.13	4.33	3.82

Here, ρ_1=760kg/m^3, η=3.2 x 10^{-4}kg/ms

TABLE IV: SIZE OF PARTICLES OR AIR BUBBLES OF BENZENE (20^{o}C)

Actual velocity v (m/sec)	(ρ_2 - ρ_1) kg/m^3				
	878	1500	2500	3500	4500
	Radius R (μm)				
5.37E-05	4.27	3.26	2.53	2.14	1.89
7.18E-05	4.94	3.77	2.93	2.47	2.18
8.30E-05	5.31	4.06	3.15	2.66	2.35
1.00E-04	5.83	4.46	3.46	2.92	2.58
1.05E-04	5.97	4.57	3.54	2.99	2.64
1.07E-04	6.03	4.61	3.57	3.02	2.66
1.14E-04	6.23	4.76	3.69	3.12	2.75
1.24E-04	6.49	4.97	3.85	3.25	2.87
1.44E-04	7	5.35	4.15	3.5	3.09
1.63E-04	7.44	5.7	4.41	3.73	3.29
1.69E-04	7.58	5.8	4.49	3.8	3.35
1.77E-04	7.76	5.93	4.6	3.89	3.43
2.12E-04	8.49	6.49	5.03	4.25	3.75
2.21E-04	8.67	6.63	5.14	4.34	3.83
2.28E-04	8.8	6.74	5.22	4.41	3.89
2.42E-04	9.07	6.94	5.38	4.54	4.01
2.51E-04	9.24	7.07	5.47	4.63	4.08
2.79E-04	9.74	7.45	5.77	4.88	4.3
2.86E-04	9.86	7.54	5.84	4.94	4.36
3.54E-04	10.97	8.39	6.5	5.49	4.85

Here, ρ_1=879kg/m^3, η=6.5 x 10^{-4}kg/ms

TABLE V: SIZE OF PARTICLES OR AIR BUBBLES OF PETROL(20^{o}C)

Actual velocity v (m/sec)	(ρ_2 - ρ_1) kg/m^3				
	729	1500	2500	3500	4500
	Radius R (μm)				
4.38E-05	4.07	2.84	2.2	1.86	1.64
5.02E-05	4.36	3.04	2.35	1.99	1.75
6.71E-05	5.04	3.51	2.72	2.3	2.03
1.08E-04	6.39	4.45	3.45	2.92	2.57
1.24E-04	6.85	4.77	3.7	3.12	2.76
1.53E-04	7.6	5.3	4.11	3.47	3.06
1.66E-04	7.92	5.52	4.28	3.61	3.19
1.81E-04	8.27	5.77	4.47	3.77	3.33
1.97E-04	8.63	6.02	4.66	3.94	3.47
2.21E-04	9.14	6.37	4.94	4.17	3.68

Here, ρ_1=730/m^3, η=6 x 10^{-4}kg/ms

VII. CONCLUSION

In the present work we have described the nature origin of dynamic fringes or moving fringes created by tiny moving macro-sized particles and air bubbles in a liquid. It has been shown conclusively that the speed and the nature of the moving fringes are different for different liquids. In the experimental arrangement we have used a He-Ne (5mW, 6328Å) or Argon-ion (500mW, 5145 Å) laser. A laser beam is incident on the lower part of a cylindrical test tube containing a particular liquid, which is transparent and also relatively dust free. Moving fringes are projected on the screen at a distance of 2m to 4m away from the sample tube. The video images of the fringes have been worked out in detail. Graphs plotted between numbers of fringes versus their speeds have exhibited distributions which are analogous to the Maxwell-Boltzman type of distribution. Tables containing data for nine samples are not included for brevity.

ACKNOWLEDGEMENT

Author is thankful to Prof. G.D. Baruah for helpful discussion and also Dr. Dip Saikia, Principal of Digboi College for granting leaves to attend the conference.

REFERENCES:

[1] J. J. Bertin, *Aerodynamics for Engineers*, 4th edition, Prentice Hall, 2001.
[2] F. Drust, A. Melling, and J. H. Whitelaw, *Principles and Practice of Laser Doppler Anemometry*, 2nd edition, London: Academic Press, 1981.
[3] J. H. Shames, *Mechanics of Fluids*, Third edition, New York: McGraw Hill, 1992.
[4] B.-H. Yuan, X.-D. Sun, Z.-X. Zhou *et al*., *J. App. Phys.*, vol. 89, no. 11, pp. 5881-5888, Jun-2001.
[5] P. Refregier, L. Solymar, H. Rajbenbach, and J. P. Huignard, *J. App. Phys*., vol. 58, no. 45, 1985.
[6] S. Ducharme, J. C. Scott, R. J. Twieg, and W. E. Moemer, *Phys. Rev. Lett.*, vol. 66, no. 1846, 1991.
[7] J. S. Schildkraut and A. V. Buettner, *J. App. Phys*., vol. 72, no. 1888, 1992.
[8] J. S. Schildkraut and Y. Cui, *J. App. Phys*., vol. 72, no. 5055, 1992.
[9] B. Yuan, X. Sun, C. Hou, Y. Li, Z. Zhou, Y. Jiang, and C. Li, *J. App. Phys*., vol. 88, no. 5562, 2000.
[10] Y. Cui, B. Suoedek, and N. Cheng, *J. App. Phys*., vol. 85, no. 38, 1999.
[11] M. MacDonald, L. Paterson, W. Sibbet and K. Dholakia, Optic Express, Vol. 10, No. 16, P. 845, (Aug-2002).
[12] D. Haubrick, M. Donseifer, and R. Wynands, "Lossless beam combiners for nearly equal Laser frequencies," *Rev. Sci. Inst*., vol. 71, no. 338, 2000.
[13] K. M. Adam, A. Steinbach, and C. F. Wieman, "A narrow band tunable Diode-Laser System with grating feedback and a saturated absorption Spectrometer for Cs and Rb," *Am., J. Phys*., vol. 60, no. 1098, 1992.
[14] S. Kuhr, W. Alt, D. Schrader, M. Muller, V. Gomer, and D. Meschede, "Deterministic Delivery of single Atom," *Science*, vol. 293, no. 278, 2001.
[15] A. E. Chiou, W. Wang, G. J. Snek. J. Hong, and M. W. Berns, "Interferometric Optical Tweezers," *Opt. Comm*., vol. 133, no. 7, 1997.
[16] M. MacDonald, L. Paterson, W. Sibbett, P. E. Bryant, and K. Dholakia, "Trapping and manipulation of law index particles in a two dimensional interferometric optical drop," *Opt. Lett*., vol. 26, no. 863, 2001.
[17] M. MacDonald, K. Volke-Sepulveda, L. Paterson, J. Arit, W. Sibbett, and K. Dholakia, " Revolving interference patterns for the rotation of optically trapped particles," *Opt. Comm*., vol. 201, no. 21, 2002.
[18] M. MacDonald, K. Volke-Sepulveda, L. Paterson, J. Arit, W. Sibbett, and K. Dholakia, "*Creation and Manipulation of Three-Dimensional Optically trapped Structures*," Science, vol. 296, no. 1101, 2002.
[19] L. Paterson, M. MacDonald, J. Arte, W. Sibbett, P.E. Bryant, and K. Dholakia, "Controlled rotation of Optically Trapped Microscopic Particles," *Science*, vol. 292, no. 912, 2001.
[20] B. A. Garetz, "Angular Doppler Effect," *JOSA Lett*., vol. 71, no. 609, 1981.
[21] I. Bialynicki-Birula and Z. Bialinicki-Birula, "Rotational Frequency shift," *Phys. Rev. Lett*., vol. 78, no. 2539, 1997.
[22] R. Simon, H. J. Kimble, and E. C. G. Sudarshan, "Evolving Geometric Phase and its Dynamical Manifestations as a Frequency shift., An Optical Experiment", *Phys. Rev. Lett*., vol. 61, no. 19, 1988.
[23] D. Schrader, S. Kuhr, W. Alt, M. Muller, V. Gomer, and D. Meshede, "A Optical Conveyer belt for single neutral atoms," *App. Phys. B*, vol. 73, no. 819, 2001.
[24] B. Ward, "Interferometry and the Doppler Effect," *A J. Mod, Opt*., vol. 44, no. 221, 1997.
[25] C. F. Buhrer, D. Baird, and E. M. Conwell, "Optical Frequency shifting by the electromagnetic effect," *Appl. Phys. Lett*., vol. 1, no. 46, 1962.
[26] F. Barone, R. De. Rosa *et al*., "Real time digital Control of Interferometer by mechanical modulation technique," *App. Opt*., vol. 33, no. 34, p. 7846, 1994.
[27] A. A. Freshi and J. Frejlich, "Adjustable Phase control in stabilized frequency," *Opt. Lett.*, vol. 20, no. 6, p. 635, 1995.
[28] A. M. Ben *et al*., "Self Adaptation in Vibrating Soap Film," *Phys. Rev. Lett*., vol. 82, no. 3847, 1999.
[29] G. Phaninsic, "Water Drop Projector," *The Phys. Teach.*, vol. 39, no. 18, 2002.
[30] W. O. Williams, "Glass tubing microscope," *The Phys. Teach*., vol. 17, no. 204, 1979.

Chandan Siam is an asst. professor of Physics, Digboi College, Assam, India. He did M.Sc. in physics in 1994 and Ph.D. in 2008 from Dibrugarh University. His specialization in M.Sc. is solid state physics and research activities in the field of laser physics. He published 8 numbers of research papers in various national and international research journals. He is a life member of *Indian Laser Association, Assam Science Society and Laser and Spectroscopic Society of India.*